

Multi-scale approach for self-Assembly and protein folding

Oriol Vilanova¹, Valentino Bianco², and Giancarlo Franzese^{1*}

¹*Secció de Física Estadística i Interdisciplinària–Departament de Física de la Matèria Condensada, Facultat de Física & Institute of Nanoscience and Nanotechnology (IN2UB), Universitat de Barcelona, Martí i Franquès 1, 08028 Barcelona, Spain and*

²*Computational Physics Group, Faculty of Physics, Universität Wien, Sensengasse 8/10, 1090 Vienna, Austria*

(Dated: March 12, 2022)

We develop a multi-scale approach to simulate hydrated nanobio systems under realistic conditions (e.g., nanoparticles and protein solutions at physiological conditions over time-scales up to hours). We combine atomistic simulations of water at bio-interfaces (e.g., proteins or membranes) and nano-interfaces (e.g., nanoparticles or graphene sheets) and coarse-grain models of hydration water for protein folding and protein design. We study protein self-assembly and crystallization, in bulk or under confinement, and the kinetics of protein adsorption onto nanoparticles, verifying our predictions in collaboration with several experimental groups. We try to find answers for fundamental questions (Why water is so important for life? Which properties make water unique for biological processes?) and applications (Can we design better drugs? Can we limit protein-aggregations causing Alzheimer? How to implement nanotheranostic?). Here we focus only on the two larger scales of our approach: (i) The coarse-grain description of hydrated proteins and protein folding at sub-nanometric length-scale and milliseconds-to-seconds time-scales, and (ii) the coarse-grain modeling of protein self-assembly on nanoparticles at 10-to-100 nm length-scale and seconds-to-hours time-scales.

I. INTRODUCTION

Self-assembly, driven by non-covalent interactions like van der Waals and hydrogen bonds, fulfills a crucial role in the supramolecular organization and assembling of the biological matter. Living beings are complex organisms where matter is self-organized on different length scales in a kind of biological network. A primary role is played by the proteins that control the majority of chemical processes in the cell. Proteins are synthesized as long polymer chains composed by hundreds of monomers, taken from 20 different amino acids. Among the huge amount of possible amino acid sequences, nature has selected those that are able to fold into specific functionalized structures, known as native protein structures. The relation between the sequence code and the native structure and the way that proteins fold represents a significant example of biological self-assembly.

A crucial aspect of the protein folding that involves the interplay with solvent is related to the hydrophobic or hydrophilic nature of the amino acids. The protein folding mechanism is dominated by the dynamics of water that drives the collapse of the hydrophobic protein core and stabilizes the tertiary protein structure [4–6]. However, many proteins exhibit a limited range of temperatures T and pressures P where they are able to maintain the native structure [7–22]. Beyond those T - and P -ranges a protein unfolds, with a consequent loss of its tertiary structure and functionality.

At high T protein unfolding is due to the thermal fluctuations that disrupt the protein structure. Open pro-

tein conformations increase the entropy S minimizing the global Gibbs free energy $G \equiv H - TS$, where H is the total enthalpy. By decreasing T proteins can crystallize but, if the nucleation of water is avoided some proteins denature [8, 10, 15, 17, 23–26]. Usually such phenomena are observed below the melting line of water, although in some cases cold denaturation occurs above the 0°, as in the case of the yeast frataxin [17].

Cold- and P -denaturation of proteins have been related to the equilibrium properties of hydration water [27–37]. However, the interpretation of this mechanism is still largely debated [38–50].

Protein denaturation is observed also upon pressurization [7, 9, 16, 22, 38]. A possible explanation of the high- P is the loss of internal cavities, sometimes presents in the folded states of proteins [48]. Denaturation at negative P has been experimentally observed [51] and simulated [37, 51, 52] recently. Pressure denaturation is usually observed at 100 MPa $\lesssim P \lesssim$ 600 MPa, and rarely at higher P unless the tertiary structure is engineered with stronger covalent bonds [14].

II. HAWLEY THEORY

In 1971, Hawley proposed a theory [53] explaining the close stability region (SR) for proteins in the T - P plane (Fig 1). The SR represents the region where a protein folds into its native conformation. Such a simple two state theory is based on the assumption that the folding (f) unfolding (u) transition is a first order phase transition and that equilibrium thermodynamics holds during the denaturation, neglecting all the details about the protein structure. Following [53] we can express the free energy difference $\Delta G \equiv G_f - G_u$ between the free en-

* gfranzese@ub.edu

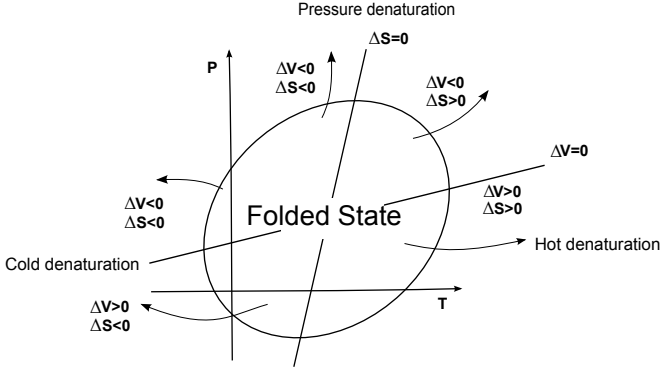


FIG. 1. Stability region of proteins according to the Hawley theory [53]. A protein is stable in its native state for temperature and pressures inside the elliptic curve. The denaturation occurs with a positive or negative variation of the total (protein plus the solvent) volume ΔV and total entropy ΔS according to the figure. Straight lines join the point where the $f \rightarrow u$ transition is isentropic or isochoric, respectively where the slope of the coexistence line is vanish or infinite. Adapted from [36].

ergy of the folded (G_f) and the unfolded (G_u) states as a quadratic function of T and P

$$\Delta G(P, T) = \frac{\Delta\beta}{2}(P - P_0)^2 + 2\Delta\alpha(P - P_0)(T - T_0) + \frac{\Delta C_P}{2T_0}(T - T_0)^2 + \Delta V_0(P - P_0) - \Delta S_0(T - T_0) + \Delta G_0 \quad (1)$$

where T_0 and P_0 are the temperature and pressure of the reference state point (ambient conditions); ΔV and ΔS are the volume and entropy variation upon unfolding respectively; $\alpha \equiv (\partial V/\partial T) = -(\partial S/\partial P)_T$ is the thermal expansivity factor, related to the isobaric thermal expansion coefficient α_P by $\alpha_P = \alpha/V$; $C_P \equiv T(\partial S/\partial T)_P$ is the isobaric heat capacity; $\beta \equiv (\partial V/\partial P)_T$ is the isothermal compressibility factor related to the isothermal compressibility K_T by the relation $K_T = (\beta/V)$ and ΔG_0 is an integration constant. Eq. (1) represents an ellipsis given the constrain

$$\Delta\alpha^2 > \Delta C_P \Delta\beta / T_0 \quad (2)$$

which is guaranteed by the different sign of ΔC_P and $\Delta\beta$ as reported by Hawley [53]. Although the calculation of Hawley is based on a Taylor expansion of the free energy variation truncated to second order. Adding more terms in the Eq. (1) results in minor corrections that do not affect the close elliptic-like coexistence curve. All in all, the Hawley model is a phenomenological theory that makes strong assumptions on the $f \rightarrow u$ process [54]. Nevertheless, its ability to describe all the denaturation mechanisms actually observed in experiments makes it a good test for models of protein unfolding.

III. A COARSE GRAIN MODEL FOR SOLVATED PROTEIN

A. Bulk water model

We present a coarse-grain model for protein water interactions based on a lattice representation of the protein, embedded in explicit water. This water model adopted is “many-body” [37, 45, 55–62].

The coarse-grain representation of the many-body interactions is based on a discretization of the available molecular volume V into a fixed number N_0 of cells, each with volume $v \equiv V/N_0 \geq v_0$, where v_0 is the water excluded volume. Each cell accommodates at most one molecule with the average O–O distance between next neighbor water molecules given by $r = v^{1/3}$. To each cell we associate a variable $n_i = 1$ if the cell i is occupied by a water molecule and it has $v_0/v > 0.5$, and $n_i = 0$ otherwise. Hence, n_i is a discretized density field replacing the water translational degrees of freedom. The Hamiltonian of bulk water is

$$\mathcal{H} \equiv \sum_{ij} U(r_{ij}) - JN_{\text{HB}}^{(b)} - J_\sigma N_{\text{coop}}. \quad (3)$$

The first term accounts for the van der Waals interaction and is modeled with a Lennard-Jones potential

$$\sum_{ij} U(r_{ij}) \equiv 4\epsilon \sum_{ij} \left[\left(\frac{r_0}{r_{ij}} \right)^{12} - \left(\frac{r_0}{r_{ij}} \right)^6 \right] \quad (4)$$

where the sum runs over all the water molecules i and j at O–O distance r_{ij} and $\epsilon \equiv 5.8$ kJ/mol. We assume $U(r) \equiv \infty$ for $r < r_0 \equiv v_0^{1/3} = 2.9$ Å that is the water molecule hard core, (water van der Waals diameter). Moreover, we apply a cutoff to the potential for $r > r_c \equiv 6r_0$.

The second term represents the directional and covalent components of the hydrogen bond (HB), where

$$N_{\text{HB}}^{(b)} \equiv \sum_{\langle ij \rangle} n_i n_j \delta_{\sigma_{ij}, \sigma_{ji}} \quad (5)$$

is the number of bulk HBs and the sum runs over the neighboring cells. $\sigma_{ij} = 1, \dots, q$ is the bonding index of molecule i with respect to the neighbor molecule j . $\delta_{ab} = 1$ if $a = b$, 0 otherwise. Each water molecule can form up to four HBs. Each HB is stable if the hydrogen atom H is in a range of $[-30^\circ; 30^\circ]$ with respect to the O–O axes. Hence, only 1/6 of the entire range of values $[0, 360^\circ]$ for the $\widehat{\text{OOH}}$ angle is associated to a bonded state, leading to the choice $q = 6$ to account correctly for the entropy variation due to HB formation and breaking. For each HB the energy decreases an amount $-J$, where $J/4\epsilon = 0.3$. According to Ref. [55], a good choice for the parameters is $\epsilon = 5.5$ kJ/mol, $J/4\epsilon = 0.5$ and $J_\sigma/4\epsilon = 0.05$. For such a choice, the average HB energy is ~ 23 kJ/mol. Here, to account for the ions in solution that are always present in the cellular environment where natural

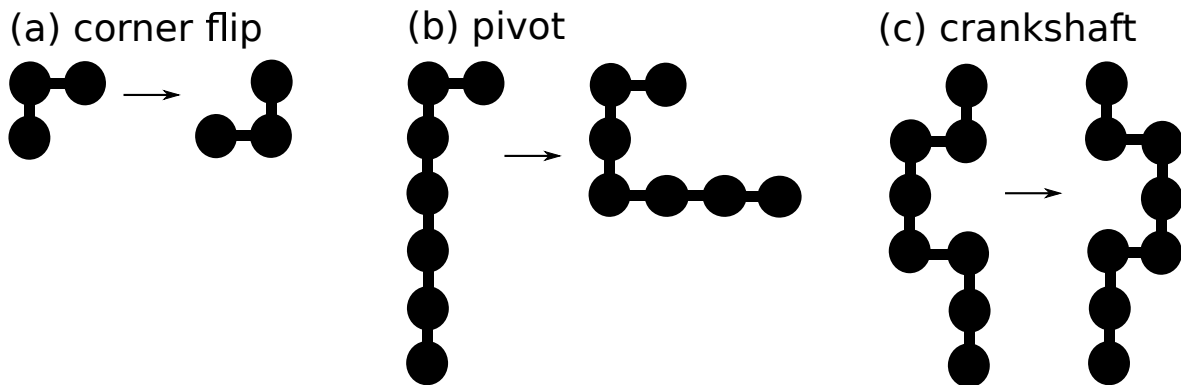


FIG. 2. Possible protein move. (a) In the *corner flip* move a monomer in a corner configuration can jump to the opposite corner. (b) In the *pivot* move we randomly choose one monomer, acting as a pivot, and rotate the shorter side chain, with respect to it. (c) The *crankshaft* move consists in choosing at random an axes passing through two monomers, and rotating the included residues.

proteins are embedded, we decrease the ratio J/J_σ , that modify the bulk phase diagram in a qualitative way similar to that induced by ions [63]. For such a choice we find that the HB energy is ~ 20 kJ/mol.

The third term in the Hamiltonian represents the cooperative interaction between the HBs. Such an effect is due to the quantum many-body interaction [64]: the formation of a new HB affects the electron distribution around the molecule favoring the formation of the following HB in a local tetrahedral structure [65]. To mimic the cooperativity of the HBs we introduce an effective interaction between the bonding indexes of a molecule

$$N_{\text{coop}} \equiv \sum_i n_i \sum_{(l,k)_i} \delta_{\sigma_{ik}, \sigma_{il}} \quad (6)$$

where $(l,k)_i$ indicates each of the six different pairs of the four indices σ_{ij} of a molecule i . The choice $J_\sigma/4\epsilon \equiv 0.05 \ll J$ guarantees the asymmetry between the two HB terms.

The formation of HBs leads to an open network of molecules, giving rise to a lower density state. We include this effect into the model assuming that, for each HB formed, the volume V increases by $v_{\text{HB}}^{(b)}/v_0 = 0.5$, corresponding to the average volume increase between high-density ices VI and VIII and low-density (tetrahedral) ice Ih. We assume that the HBs do not affect the distance r between first neighbour molecules, consistent with experiments [65]. Hence, the HB formation does not affect the $U(r)$ term.

The total bulk volume $V^{(b)}$ is

$$V^{(b)} \equiv Nv_0 + N_{\text{HB}}^{(b)}v_{\text{HB}}^{(b)}. \quad (7)$$

B. Modeling protein-water interplay

The protein is modeled as a hydrophobic self-avoiding lattice polymer and it is embedded into the cell partition

of the system. Despite its simplicity, lattice protein models are still widely used in the contest of protein folding [28, 29, 35, 37, 66, 67] because of their versatility and the possibility to better understand many mechanisms of the protein dynamics. Each protein residue (polymer bead) occupies one cell, without affecting its volume. In the present study, we do not consider the presence of cavities into the protein structure.

To simplify the discussion, we assume that no residue-residue interactions occur and that the residue-water interaction vanishes. This implies that the protein has several ground states, all with the same maximum number n_{max} of residue-residue contacts. Our results holds also when such interactions are restored [37]. Here we adopt the symbol Φ to refer to hydrophobic residues. The protein interface affects the water-water properties in the hydration shell, here we define it as the layer of first neighbor water molecules in contact with the protein. There are many numerical and experimental evidences supporting the hypothesis that water-water HBs in the hydration shell are more stable and more correlated with respect to bulk HBs [68–72]. We account for this by replacing J of Eq. (3) with $J_\Phi > J$ for water-water HBs at the Φ interface. This choice, according to Muller [73], ensures the water enthalpy compensation upon cold-denaturation [36].

In addition to the stronger/stabler water-water HBs in the Φ shell, we incorporate into the model also the larger density fluctuations at the Φ interface with respect to the bulk, observed in water hydrating Φ solutes [43, 70]. Such an increase of density fluctuations results in a Φ hydration shell that, at ambient pressure, is more compressible than bulk water. Although it is still matter of debate whether the average density of water at the Φ interface is larger or smaller with respect to the average bulk water density [74–78], there is evidence showing that such density fluctuations reduce upon pressurization [43, 70, 79, 80]. Hence, if we attribute this P -dependence of the Φ shell density to the interfacial HB properties, we

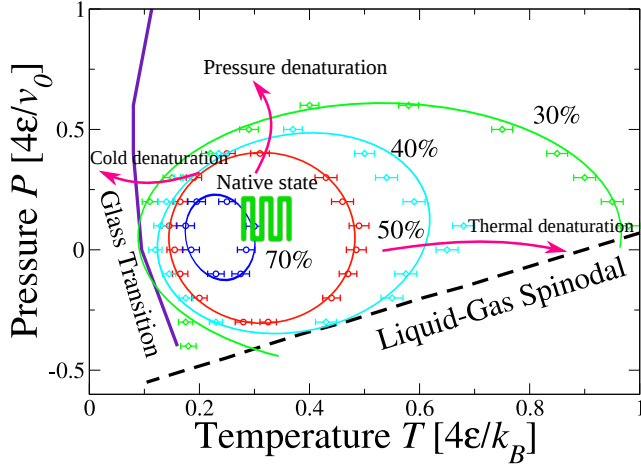


FIG. 3. $P - T$ stability region of the protein, calculated with Monte Carlo simulations. The symbols mark the state points where the protein has the same average residue-residue contact's number $n_{\text{rr}}/n_{\text{max}} = 30\%$, 40% , 50% and 70% , corresponding to different percentage of compactness. Elliptic lines are guides for the eyes. The “glass transition” line defines the temperatures below which the system does not equilibrate. The spinodal line marks the stability limit of the liquid phase at high P with respect to the gas at low P ; k_B is the Boltzmann constant.

can assume that the average volume associated to HBs formed in the Φ shell is

$$v_{\text{HB}}^{(\Phi)}/v_{\text{HB},0}^{(\Phi)} \equiv 1 - k_1 P \quad (8)$$

where $v_{\text{HB},0}^{(\Phi)}$ is the volume change associated to the HB formation in the Φ hydration shell at $P = 0$ and k_1 is a positive factor. According to Ref. [37], we could add other polynomial terms to the Eq. (8), although such terms would not affect our results as long as $P < 1/k_1$ [81].

The total volume V , including the contributions coming from the HBs formed in the Φ shell is

$$V \equiv Nv_0 + N_{\text{HB}}^{(b)}v_{\text{HB}}^{(b)} + N_{\text{HB}}^{(\Phi)}v_{\text{HB}}^{(\Phi)}. \quad (9)$$

where $N_{\text{HB}}^{(\Phi)}$ is the number of HBs in the Φ shell.

In the following we fix $k_1 = 1v_0/4\epsilon$, $v_{\text{HB},0}^{(\Phi)}/v_0 = v_{\text{HB}}^{(b)}/v_0 = 0.5$ and $J_{\Phi}/J = 1.83$. Our findings are robust with respect to a change of parameters.

C. Simulation details

We study proteins with 30 residues using Monte Carlo simulations in the isobaric-isothermal ensemble, i.e. at constant P , constant T and constant number of particles. All the simulations start with a protein in a completely folded conformation. The water bonding indexes σ are equilibrated using a cluster algorithm. The protein

is equilibrated using corner flips, pivot and crunkshuft moves [82] (Fig 2). Along the simulation we calculate the average number of residue-residue contact points to estimate the protein compactness. For each state point we sample $\sim 10^4$ independent protein conformations.

D. Results

We assume that the protein is folded if the average number of residue-residue contacts is $n_{\text{rr}} \geq 50\% n_{\text{max}}$. In Fig. 3 we show the calculated SR for the protein, consistent with the Hawley theory [12, 53]. We observe that the SR has an elliptic shape that is preserved independently of the compactness we adopt as the reference for the folded state, underlying that the folded \rightarrow unfolded transition is a continuous process. Proteins undergo heat-, cold-, and P -unfolding. The folded protein minimizes the number of hydrated Φ residues, reducing the energy cost of the interface, as expected.

Upon increasing T at constant P , we observe that the model reproduces the expected *entropy-driven* unfolding. The entropy S increases both for the opening of the protein and for the larger decrease of water-water HBs.

Decreasing T at constant P leads to open protein conformations that minimize the Gibbs free energy. The difference in energy gain between bulk HBs and HBs at the Φ interface results in a competing mechanism. A bulk water molecule can form up to 4 HBs, while the water molecules at the Φ interface can form up to 3 HBs, although stronger. Hence, reducing the exposed protein surface maximizes the possible number of bulk HBs, while increasing the hydrated protein surface maximizes the interfacial HBs. At low T the number of HBs in the Φ shell saturates and the only way for the system to further minimize the internal energy is by increasing $N_{\text{HB}}^{(\Phi)}$, i.e. by unfolding the protein. Hence, the cold denaturation is an *energy-driven* process.

Upon an isothermal increase of P the protein denatures. We find that this change is associated to a decrease of $N_{\text{HB}}^{(b)}$ and an increase of $N_{\text{HB}}^{(\Phi)}$ leading to a net decrease of V at high P , as a consequence of the compressible Φ shell, Eqs. (8). At high P , the PV term of the Gibbs free energy dominates the $f \rightarrow u$ process. Hence, the water contribution to the high- P denaturation induces a *density-driven* process, resulting in a denser Φ shell with respect to the bulk.

Finally, lowering P toward negative values results in a negative contribution $(Pv_{\text{HB}}^{(\Phi)} - J_{\Phi})N_{\text{HB}}^{(\Phi)}$, leading to a decrease in enthalpy when the protein opens up and $N_{\text{HB}}^{(\Phi)}$ increases. Therefore we find that at negative P the denaturation process is *enthalpy-driven*.

By varying the parameters $v_{\text{HB}}^{(\Phi)}$ and J_{Φ} we find that the first is relevant for the P -denaturation, as we expected because it dominates the volume contribution to the Gibbs free energy, while the second affects the stability range in T . Both effects combine in a non-trivial

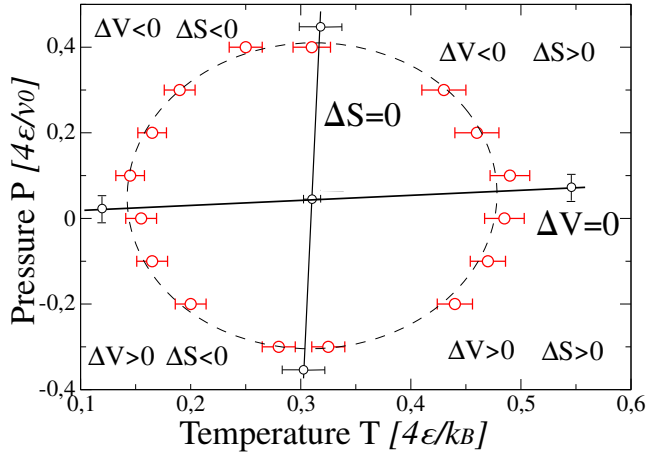


FIG. 4. Volume change ΔV and entropy change ΔS for the $f \rightarrow u$ process in the $T - P$ plane. Solid lines connect state points with isochoric $\Delta V = 0$ and isentropic $\Delta S = 0$ denaturation. Red points mark the SR, adopted from Fig. (3). The loci $\Delta V = 0$ and $\Delta S = 0$ have a positive slope and intersect the SR at the turning points with $dT/dP|_{\text{SR}} = 0$ and $dT/dP|_{\text{SR}} = \infty$ respectively.

way to regulate the SR, shifting, shrinking and dilating the SR, although the elliptic shape is preserved [81].

We can estimate also the entropy change and volume change, respectively indicated with ΔS and ΔV , during the $f \leftrightarrow u$ process. First, we calculate the average volume of the unfolded-completely stretched-protein V_u and of the folded-maximum compactness-protein V_f in a wide range of T and P , equilibrating water around the fixed protein conformations. From the difference $\Delta V \equiv V_f - V_u$ we calculate ΔS using the Clapeyron relation $dP/dT = \Delta S/\Delta V$ applied to the SR [53]. The Clapeyron equation holds, in principle, only along first order phase transitions. Though the $f \leftrightarrow u$ process is not necessary a phase transitions, the calculation of ΔS and ΔV represents a good model test to compare our model results with the Hawley's theory [53]. In Fig. 4 we show that our findings match with the theoretical predictions: T -denaturation is accompanied by a positive entropy variation $\Delta S > 0$ at high T and an entropic penalty $\Delta S < 0$ at low T ; P -denaturation is accompanied by a decrease of volume $\Delta V < 0$ at high P and an increase of volume $\Delta V > 0$ at low P . In particular, at $P = 0.3(4\epsilon/v_0)$, corresponding to ≈ 500 MPa, we find that $\Delta V \approx -2.5v_0$, hence $|P\Delta V| = 0.75(4\epsilon) \approx 17$ kJ/mol, very close to the typical reported value of 15 kJ/mol [16].

Therefore our coarse-grain model allows to understand how water contributes to the temperature- and pressure-denaturation of proteins. Accounting for stronger and more stable HBs in the hydrophobic hydration shell with respect to the bulk and for a more compressible hydrophobic hydration shell our model reproduces a close stability region for proteins with the expected elliptic-like shape in the $T - P$ plane, consistent with theory

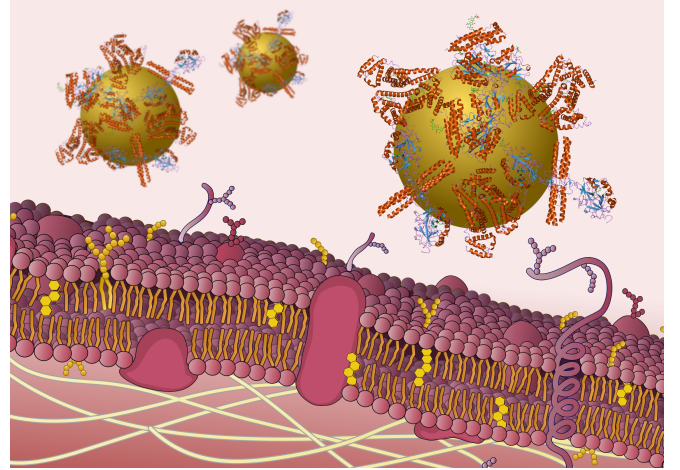


FIG. 5. Pictorial representation of the NP-‘Protein corona’ complex near a cellular membrane

[53]. We find that cold denaturation is energy-driven, while unfolding at high pressures and negative pressures are density- and enthalpy-driven by water, respectively.

IV. PROTEIN ADSORPTION ONTO NPS: KINETICS OF THE PROTEIN-CORONA FORMATION

Nanoparticles (NPs) are small scale objects with dimensions in the range from 1 nm (10^{-9} m) up to 100 nm. The main feature of these particles rely on the fact that some of their properties differ completely from the bulk material they are made of. Furthermore, their properties strongly depend on the particle size. Due to their small size, the surface to volume ratio of NPs is much higher than that of macroscopic objects. This feature, combined with the high surface free energy of NPs, confers NPs a high level of chemical reactivity.

The NPs particular interactions with biological systems make them very promising tools for medical applications and could allow to simultaneously perform therapeutics and diagnostics (*theranostics*) [83–85]. In particular, experiments show that NPs are able to cross cellular barriers, including the strongest defense we have in our body, the blood-brain-barrier. Therefore, the fact that NPs interact directly with the biological machinery [86] represent an opportunity to deliver drugs to specific targets hidden in the most inaccessible spots within the cells for treating illnesses that challenge us, such as cancer or neurodegenerative diseases [87].

In the last years, industry has started to produce NPs at a large scale, with an increasing rate, due to their industrial, commercial and medical applications. Thousands of commercial products, such as textiles, cosmetics or paints contain NPs, and nanomaterials are nowadays used in medical treatments, electronics, or food. In order to keep producing and using them at the industrial

scale safely, many experimental studies [88] of the nanotoxicology impact [89] of specific NPs have started to evaluate the hazard of exposing the environment, living beings and humans to them [90–93].

Yet, very little is known about the mechanisms regulating the interactions of NPs with biological systems [94]. Acquiring such knowledge would allow us to predict if the interaction of such small-scale materials with living organisms would potentially be dangerous before even performing elaborated experiments.

It has been confirmed that NP’s absorb proteins and other biomolecules from the environment forming a complex that is known as the “protein corona” (Fig.5) [95–100]. Certain proteins are also able to prevent the adsorption of other molecules, or to modify the chemical properties of the NP surface, and even to determine the path and final localization of the NP in a living organism [84, 101].

Material surfaces exposed to biological environments are commonly modified by the adsorption of biomolecules, such as proteins and lipids, already present in solution. It has been shown that the cellular response to any material in a biological medium is mediated by the adsorbed biomolecular layer, rather than the bare material itself [96, 97]. For this reason, the scientific community has focused its attention to the fact that NP interactions with living organisms must be also mediated by the adsorbed protein layer [102, 103]. It is now understood that the biological identity of the NP is characterized by the distribution of the distinct adsorbed proteins on its surface [104–107]. This collection of adsorbed biomolecules is in fact dynamic and evolves in time [96–98, 100, 103]. The effective particle made by the protein-NP-corona is essential to understand how NPs interact with cells in biological media [102]. Our aim is to understand and explain how the interactions between biological macromolecules and NPs in solution leads to the formation of the effective particle and to its evolution over time scales that are relevant in the biological context.

In the following we address the establishment of a theoretical framework and the determination of the key features that could give a simple, but complete, picture of protein-NP interactions. We focus on parameters that describe the NP surface at the molecular level, such as curvature, charge or surface chemistry, that determine which kinds of proteins ends up binding from a complex biological fluid, e.g., blood plasma or cell media [106].

The adoption of a multi-scale approach in this respect is particularly suitable because it provides the theoretical framework to study a variety of aspects that occur at different length- and time-scales, ranging from the atomistic scale ($\sim 0.1\text{nm}$ and $\sim 1\text{ns}$) to the mesoscale ($\sim 1\mu\text{m}$ and $\sim 100\text{s}$). We, therefore, first establish phenomenological models for protein-protein and protein-NP interactions, in solvent [108]. Next, we validate these models with, at least, two types of NPs using available experimental data [109]. Finally we perform predictions, based on our theoretical models, and we test them by comparing with ex-

perimental data. In particular, experimentally checking the kinetics and the protein corona composition allows us to assess the predictive power of the models when we use only our knowledge on physico-chemical properties of the nanomaterial and the environmental conditions [110].

V. METHODOLOGY

A. Multi-scale modeling

For the purpose of developing this research we make use of state-of-the-art techniques of computational and theoretical modeling. Thereby, we adopt a multi-scale approach to carry out this study. Multi-scale modeling is based on the idea that each specific problem is characterized by multiple scales of time and space. There is a need to consider every scale to understand the whole picture, given the relevance of different mechanisms occurring at each scale. This approach is particularly appropriate for the case of biological systems at the nanoscale, such as the interactions of NPs with macromolecules in presence of water. In this situation, the length scales range from angstroms to micrometers while the time scales span more than ten orders of magnitude.

We separate our analysis into different levels of description, based on the observation that each length scale has an associated time scale. By these means, each level of description is related to a range of length and time scales that partially overlap with the consecutive levels. To this end, each level is characterized by specific phenomena, which can be useful to understand features of other, maybe more complex, phenomena at higher levels of description. In our case, we consider the following levels of description: (i) the molecular and macromolecular level, ranging from 1 \AA to 100 nm and from 10 fs to $1\mu\text{s}$, and (ii) the mesoscale level, ranging from 1 nm to $1\mu\text{m}$ and from 10 ns to 1 s . The next step is to consider, for example, the problem of NP aggregation or the interaction of NPs with cellular membranes, that would span a range of length scales up to $100\mu\text{m}$ and time-scales up to hours.

B. Theoretical framework

We make use of suitable computational and theoretical techniques to approach each level of description. The smaller scales are characterized by the explicit consideration of water molecules in the solvent, as mediators of the processes that occur at the macromolecular scale. However, dealing with explicit solvent models hampers the efficiency of computation in a dramatic way. This is why we adopt the coarse-grain model of water introduced in the previous sections [55, 58, 61] to describe the macromolecule-solvent interactions [37]. This is a convenient strategy that allows for wider and more efficient options to explore these systems. The model can be efficiently simulated using the Monte Carlo (MC) method

[55, 58, 111, 112] and can be also treated analytically, allowing us to reach a deeper understanding of the fundamental mechanisms [113–115].

At the larger scales, where we focus our attention on the interaction of NPs with solutions containing a large number of proteins, we use an implicit solvent approach. In this sense, we take into account the effects of the solvent by my means of modified dynamics and effective interactions. Therefore, we also consider the proteins and the NPs as coarse-grain objects. We adopt a Molecular Dynamics (MD) simulation scheme using Langevin dynamics (LD), that allows for the determination of the kinetic properties of the system. Moreover, we introduce a framework that describes protein-protein interactions via effective potentials, and we make use of the well established DLVO theory for colloidal dispersions in solution to describe the protein-NP interactions [110].

Finally, we develop a Non-Langmuir Dynamical Rate Equation (NLDRE) model which is phenomenological analytical theory to describe the protein adsorption kinetics [110]. This theory provides us tools to extrapolate the simulation results of protein adsorption obtained with MD, to much longer time-scales. With this approach we are able to predict kinetic processes over experimentally relevant time-scales of the order of several minutes, far beyond the limits of the computational capacities [110].

C. Experimental validation

The collaborative work of theorist and experimentalists is a key factor for the successful development of theoretical models with predictive capability. The experimental data is fundamental for the parametrization of the theoretical models, yet it is crucial for the validation and verification process of the theoretical predictions. To this goal we focus on a simplified version of a multicomponent protein solution as it would be the human blood plasma. In particular, we adopt a “model plasma” containing only three proteins that are representative of the extremely large number of protein forming the human blood [110]. This step is essential to design experiments suitable for comparison with simulations.

We follow a workflow where we can first measure in a controlled experimental setup all the data that are relevant for defining the phenomenological parameters of the theoretical model. In this way, the preliminary experimental results serve to calibrate the theoretical model.

Next we perform our simulations and analytic prediction based on these phenomenological input parameters. We make our calculation under conditions that can be reproduced in experiments, in simple cases with NPs in bicomponent protein solutions, for a direct comparison. Then we design a set of simple experiments to validate the simulation results obtained under identical conditions.

Finally, to test the predictive power of the theoretical tools, we consider more complex situations, such as NPs

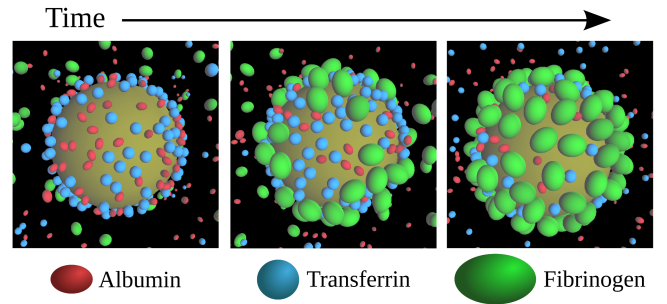


FIG. 6. Simulation snapshots at three different times for a system containing one silica NP of 100nm diameter in a solution containing Human Serum Albumin (HSA), Transferrin (Tf) and Fibrinogen (Fib). The introduction of each protein is done sequentially in three steps: HSA first, Tf second and Fib third.

in three-component solutions made of proteins that are competing for the NP surface. Under these conditions the experiments reveal a *memory effect* of the protein corona, not predicted by our initial model. As a consequence, we modify the model in a way that allows us to reproduce the effect. Although this result exposes a limit of our initial approach, it also led us to propose a mechanism to rationalize the memory effect. Specifically, we show that to account for the memory effect it is necessary to model the self-assembly of the proteins on the NPs including irreversible structural changes [110].

D. Simulation details and results

We develop a high-performance suite of simulation codes able to run on Graphical Processing Units (GPU's) [116]. We use a molecular dynamics (MD) approach to simulate the interactions of NPs with protein solutions. We consider a simulation box with periodic boundary conditions containing one single NP fixed to the center of the box. We separate the simulation box into two regions. The inner region contains the NP, while we use the external region as a reservoir to control the protein concentration inside the inner region [110]. We treat the solvent in an implicit way, by introducing a coarse-grain protein-protein and protein-NP interaction model using continuous shouldered potentials [108, 117, 118]. We also adopt a Langevin dynamics (LD) integration scheme to take into account the collisions with the solvent molecules for the correct diffusion of the proteins.

We follow a sequential protocol to insert different kinds of proteins at selected times during a simulation. For example, in Fig.6 we show three snapshots of a simulation containing a 100nm diameter silica (SiO_2) NP at 0.1 mg/ml in a protein solution of Human Serum Albumin (HSA), Transferrin (Tf) and Fibrinogen (Fib). The first snapshot shows the equilibrium state after introducing HSA at 0.07 mg/ml and Tf at 0.07 mg/ml to the sys-

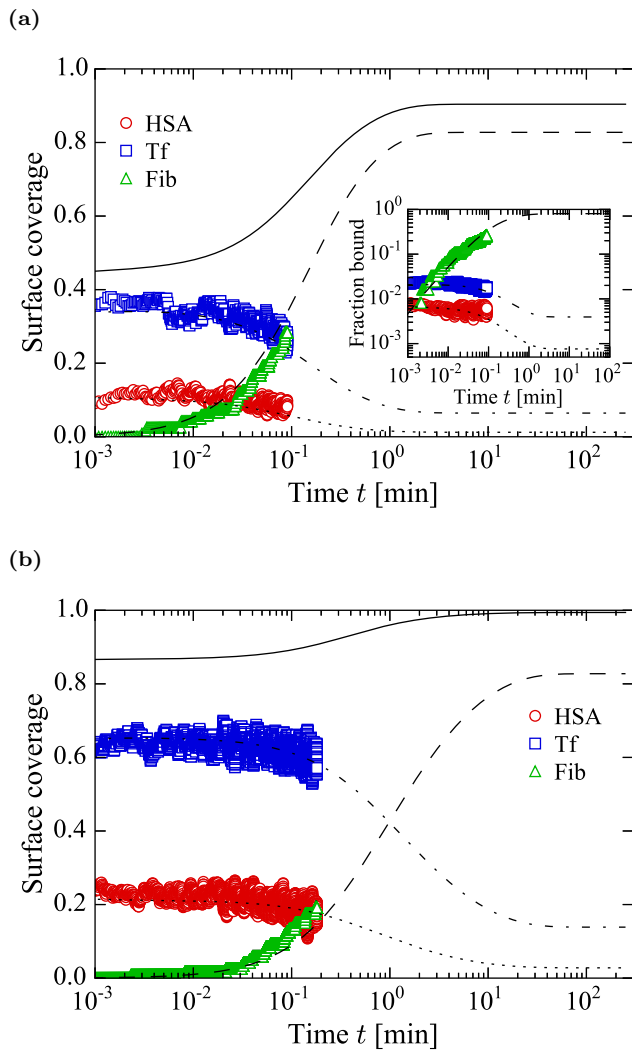


FIG. 7. Simulation results (symbols) and analytical extrapolation (lines) using NLDRE of the protein corona kinetics in a system containing 100nm silica NPs at 0.1 mg/ml in a protein solution containing HSA (red circles), Tf (blue squares) and Fib (green triangles) at different concentrations. The NPs are initially incubated in a solution containing HSA and Tf, with the subsequent introduction of Fib at 0.005 mg/ml. We also show the analytical extrapolation using the NLDRE theory to the simulation data for each protein (dashed lines), and the total surface coverage (solid lines). a) NP surface coverage after incubation in a solution of HSA at 0.07 mg/ml and Tf at 0.07 mg/ml, inset: Fraction bound of proteins shown for comparison with the surface coverage. b) NP surface coverage after incubation in a solution of HSA at 3.5 mg/ml and Tf at 3.5 mg/ml.

tem, at the same moment that we introduce Fib at 0.005 mg/ml. The second snapshot is a transient state, where Fib begins adsorbing to the NP surface. In the third snapshot we show how the high affinity of Fib allows it to displace HSA and Tf proteins from the surface, while the system has not yet reached equilibrium because this is a kinetically slow process (Fig.7a).

In Fig.7 we show the effect of increasing the concentration of the proteins during the incubation step to the adsorption kinetics of the third protein. In panel a) the NP is incubated in a solution of HSA and Tf at a low concentration of 0.07 mg/ml each, and we introduce Fib at 0.005 mg/ml which is a protein with a much higher surface affinity. We make use of our NLDRE to fit the parameters to the simulation data and we extrapolate the adsorption kinetics to much longer time-scales. In panel b) we show the adsorption kinetics of a system where we initially incubate the NP in a solution of HSA and Tf at a much higher concentration of 3.5 mg/ml each. Using the analytical extrapolation to the simulation data we find that the Fib adsorption kinetics are at least 1 order of magnitude slower compared to the previous situation.

VI. CONCLUSIONS

We combine theory with experiments to introduce a new framework consisting in experiment design supported by computational simulations and theoretical models as a methodology to obtain reliable predictive results for protein folding and protein-NP self-assembly.

We establish a multi-scale modeling approach to deal with the different phenomenologies characteristic to each level of description. Based on atomistic Molecular Dynamics simulations over nanoseconds up to microseconds time-scales, we define a coarse-grain water model that allows us to simulate hydrated systems [119] at length- and time-scales that are relevant for biological processes. This model allows us to study by Monte Carlo simulations protein structural changes and folding-unfolding events [37]. We recently extended this approach to study protein design [120].

With this in mind, we introduce a set of computational tools (BUBBLES [116]) that allows us to study phenomenological protein-protein and protein-NP interactions [108] with Langevin Dynamics simulations up to the time scale of seconds. Next we introduce a phenomenological theory based on rate equation (NLDRE) with which we can extrapolate our simulation results to time scales of hours, allowing us direct comparison with the experimental results.

In particular, we first study the protein corona formation for a simple system of polystyrene NPs in a solution containing only a single kind of proteins (Transferin). We introduce many-body interactions to explain the multilayer adsorption mechanism, the protein corona kinetics, and the soft-corona/hard-corona characterization [109].

Next, we study more complicated systems by introducing NPs in solutions made of multiple types of proteins, choosing a set of proteins that compete for the NP surface. This allows for the emergence of competitive protein adsorption and assembly on top of the NP, a rich and complex playground that we exploit to discover and understand new and unexpected features [110].

ACKNOWLEDGEMENT

We are thankful to M. Bernabei, C. Calero, L. E. Coronas, F. Leoni, N. Pagès, and A. Zantop for helpful discus-

sions. O.V. and G.F. acknowledge the support of Spanish MINECO grant FIS2012-31025 and FIS2015-66879-C2-2-P. I. C. acknowledges the support from the Austrian Science Fund (FWF) Grant P 26253-N27. V.B. acknowledges the support of the FWF Grant 2150-N36 and P 26253-N27.

-
- [1] Yaakov Levy and José N Onuchic. Water and proteins: a love-hate relationship., *Proceedings of the National Academy of Sciences of the United States of America*, 101(10):3325–6, March 2004.
 - [2] Yaakov Levy and José N Onuchic. Mechanisms of protein assembly: Lessons from minimalist models, *Accounts Of Chemical Research*, 39(2):135–142, 2006.
 - [3] Tanya M Raschke. Water structure and interactions with protein surfaces., *Current opinion in structural biology*, 16(2):152–159, April 2006.
 - [4] Yaakov Levy and José N Onuchic. Water and proteins: a love-hate relationship., *Proceedings of the National Academy of Sciences of the United States of America*, 101(10):3325–6, March 2004.
 - [5] Yaakov Levy and José N Onuchic. Mechanisms of protein assembly: Lessons from minimalist models, *Accounts Of Chemical Research*, 39(2):135–142, 2006.
 - [6] Tanya M Raschke. Water structure and interactions with protein surfaces., *Current opinion in structural biology*, 16(2):152–159, April 2006.
 - [7] Adam Zipp and Walter Kauzmann. Pressure denaturation of metmyoglobin, *Biochemistry*, 12(21):4217–4228, October 1973.
 - [8] Peter L. Privalov. Cold denaturation of proteins, *Crit Rev Biochem Mol Biol*, 25(4):281–305, 1990.
 - [9] Gerhard Hummer, Shekhar Garde, Angel E García, Michael E Paulaitis, and Lawrence R Pratt. The pressure dependence of hydrophobic interactions is consistent with the observed pressure denaturation of proteins, *Proceedings of the National Academy of Sciences*, 95(4):1552–1555, 1998.
 - [10] Filip Meersman, László Smeller, and Karel Heremans. Pressure-assisted cold unfolding of proteins and its effects on the conformational stability compared to pressure and heat unfolding, *High Pressure Research*, 19(1-6):263–268, 2000.
 - [11] Michael W Lassalle, Hiroaki Yamada, and Kazuyuki Akasaka. The pressure-temperature free energy-landscape of staphylococcal nuclease monitored by (1)H NMR., *Journal of molecular biology*, 298(2):293–302, April 2000.
 - [12] László Smeller. Pressure-temperature phase diagrams of biomolecules, *Biochimica et Biophysica Acta (BBA) - Protein Structure and Molecular Enzymology*, 1595(1-2):11–29, March 2002.
 - [13] Heinz Herberhold and Roland Winter. Temperature- and Pressure-Induced Unfolding and Refolding of Ubiquitin: A Static and Kinetic Fourier Transform Infrared Spectroscopy Study , *Biochemistry*, 41(7):2396–2401, February 2002.
 - [14] Harald Lesch, Hans Stadlbauer, Josef Friedrich, and Jane M Vanderkooi. Stability Diagram and Unfolding of a Modified Cytochrome c: What Happens in the Transformation Regime?, *Biophysical Journal*, 82(3):1644–1653, March 2002.
 - [15] Revanur Ravindra and Roland Winter. On the Temperature-Pressure Free-Energy Landscape of Proteins, *Chem Phys Chem*, 4(4):359–365, April 2003.
 - [16] Filip Meersman, Christopher M Dobson, and Karel Heremans. Protein unfolding, amyloid fibril formation and configurational energy landscapes under high pressure conditions., *Chemical Society reviews*, 35(10):908–17, October 2006.
 - [17] Annalisa Pastore, Stephen R Martin, Anastasia Politou, Kalyan C Kondapalli, Timothy Stemmler, and Piero A Temussi. Unbiased Cold Denaturation: Low- and High-Temperature Unfolding of Yeast Frataxin under Physiological Conditions, *Journal of the American Chemical Society*, 129(17):5374–5375, 2007.
 - [18] Johannes Wiedersich, Simone Köhler, Arne Skerra, and Josef Friedrich. Temperature and pressure dependence of protein stability: the engineered fluorescein-binding lipocalin FluA shows an elliptic phase diagram., *Proceedings of the National Academy of Sciences of the United States of America*, 105(15):5756–61, April 2008.
 - [19] Akihiro Maeno, Hiroshi Matsuo, and Kazuyuki Akasaka. The pressure-temperature phase diagram of hen lysozyme at low pH, *BIOPHYSICS*, 5:1–9, March 2009.
 - [20] Judit Somkuti, Zsolt Mártonfalvi, Miklós S Z Kellermayer, and László Smeller. Different pressure-temperature behavior of the structured and unstructured regions of titin., *Biochimica et biophysica acta*, 1834(1):112–8, January 2013.
 - [21] Judit Somkuti, Sriyans Jain, Srinivasan Ramachandran, and László Smeller. Folding-unfolding transitions of Rv3221c on the pressure-temperature plane, *High Pressure Research*, 33(2):250–257, June 2013.
 - [22] Nathaniel V Nucci, Brian Fuglestad, Evangelia A Athanasoula, and A Joshua Wand. Role of cavities and hydration in the pressure unfolding of T4 lysozyme., *Proceedings of the National Academy of Sciences of the United States of America*, 111(38):13846–51, September 2014.
 - [23] Yuri V. Griko, Peter L. Privalov, Julian M. Sturtevant, and Sergey Yu. Venyaminov. Cold denaturation of staphylococcal nuclease., *Proceedings of the National Academy of Sciences*, 85(10):3343–3347, May 1988.
 - [24] Koen Goossens, László Smeller, Johannes Frank, and Karel Heremans. Pressure-Tuning the Conformation of Bovine Pancreatic Trypsin Inhibitor Studied by Fourier-Transform Infrared Spectroscopy, *European Journal of Biochemistry*, 236(1):254–262, 1996.

- [25] David P Nash and Jiri Jonas. Structure of the pressure-assisted cold denatured state of ubiquitin, *Biochemical and biophysical research communications*, 238(2):289–291, 1997.
- [26] David P Nash and Jiri Jonas. Structure of Pressure-Assisted Cold Denatured Lysozyme and Comparison with Lysozyme Folding Intermediates, *Biochemistry*, 36(47):14375–14383, 1997.
- [27] Paolo De Los Rios and Guido Caldarelli. Putting proteins back into water, *Physical Review E*, 62(6):8449–8452, 2000.
- [28] Manuel I Marqués, Jose M Borreguero, H. Eugene Stanley, and Nikolay V Dokholyan. Possible Mechanism for Cold Denaturation of Proteins at High Pressure, *Phys. Rev. Lett.*, 91(13):138103, 2003.
- [29] Bryan A Patel, Pablo G. Debenedetti, Frank H Stillinger, and Peter J Rossky. A Water-Explicit Lattice Model of Heat-, Cold-, and Pressure-Induced Protein Unfolding, *Biophysical Journal*, 93(12):4116–4127, 2007.
- [30] Manoj V Athawale, Gaurav Goel, Tuhin Ghosh, Thomas M Truskett, and Shekhar Garde. Effects of lengthscales and attractions on the collapse of hydrophobic polymers in water., *Proceedings of the National Academy of Sciences of the United States of America*, 104(3):733–8, January 2007.
- [31] Daniel Nettels, Sonja Müller-Späth, Frank Küster, Hagen Hofmann, Dominik Haenni, Stefan Rüegger, Luc Reymond, Armin Hoffmann, Jan Kubelka, Benjamin Heinz, Klaus Gast, Robert B Best, and Benjamin Schuler. Single-molecule spectroscopy of the temperature-induced collapse of unfolded proteins, *Proceedings of the National Academy of Sciences*, 106(49):20740–20745, 2009.
- [32] Robert B Best and Jeetain Mittal. Protein simulations with an optimized water model: cooperative helix formation and temperature-induced unfolded state collapse., *The journal of physical chemistry. B*, 114(46):14916–23, November 2010.
- [33] Sumanth N Jamadagni, Christian Bosoy, and Shekhar Garde. Designing heteropolymers to fold into unique structures via water-mediated interactions., *The journal of physical chemistry. B*, 114(42):13282–8, October 2010.
- [34] Artem V. Badasyan, Shushanik A. Tonoyan, Yevgeni Sh. Mamasakhlisov, Achille Giacometti, A. S. Benight, and Vladimir F. Morozov. Competition for hydrogen-bond formation in the helix-coil transition and protein folding., *Physical review. E, Statistical, nonlinear, and soft matter physics*, 83(5 Pt 1):051903, May 2011.
- [35] Silvina Matysiak, Pablo G. Debenedetti, and Peter J Rossky. Role of Hydrophobic Hydration in Protein Stability: A 3D Water-Explicit Protein Model Exhibiting Cold and Heat Denaturation, *The Journal of Physical Chemistry B*, 116(28):8095–8104, 2012.
- [36] Valentino Bianco, Svilen Iskrov, and Giancarlo Franzese. Understanding the role of hydrogen bonds in water dynamics and protein stability. *Journal of Biological Physics*, 38(1):27–48, 2012.
- [37] Valentino Bianco and Giancarlo Franzese. Contribution of Water to Pressure and Cold Denaturation of Proteins, *Phys. Rev. Lett.*, 115(10):108101, September 2015.
- [38] Dietmar Paschek and Angel E García. Reversible temperature and pressure denaturation of a protein fragment: a replica exchange molecular dynamics simulation study., *Physical review letters*, 93(23):238105, December 2004.
- [39] Dietmar Paschek, S Gnanakaran, and Angel E Garcia. Simulations of the pressure and temperature unfolding of an alpha-helical peptide., *Proceedings of the National Academy of Sciences of the United States of America*, 102(19):6765–70, May 2005.
- [40] Tomonari Sumi and Hideo Sekino. Possible mechanism underlying high-pressure unfolding of proteins: formation of a short-period high-density hydration shell., *Physical chemistry chemical physics : PCCP*, 13(35):15829–32, September 2011.
- [41] Ivan Coluzza. A coarse-grained approach to protein design: learning from design to understand folding. *PloS one*, 6(7):e20853, 2011.
- [42] Cristiano L Dias. Unifying microscopic mechanism for pressure and cold denaturations of proteins., *Physical review letters*, 109(4):048104, July 2012.
- [43] Payel Das and Silvina Matysiak. Direct Characterization of Hydrophobic Hydration during Cold and Pressure Denaturation, *The Journal of Physical Chemistry B*, 116(18):5342–5348, 2012.
- [44] Rahul Sarma and Sandip Paul. Effect of pressure on the solution structure and hydrogen bond properties of aqueous N-methylacetamide, *Chemical Physics*, 407(0):115–123, October 2012.
- [45] Giancarlo Franzese and Valentino Bianco. Water at Biological and Inorganic Interfaces, *Food Biophysics*, 8(3):153–169, 2013.
- [46] Sanne Abeln, Michele Vendruscolo, Christopher M Dobson, and Daan Frenkel. A simple lattice model that captures protein folding, aggregation and amyloid formation., *PloS one*, 9(1):e85185, January 2014.
- [47] Changwon Yang, Soonmin Jang, and Youngshang Pak. A fully atomistic computer simulation study of cold denaturation of a β -hairpin., *Nature communications*, 5:5773, January 2014.
- [48] Julien Roche, Jose A. Caro, Douglas R. Norberto, Philippe Barthe, Christian Roumestand, Jamie L. Schlessman, Angel E Garcia, Bertrand E García-Moreno, Catherine A. Royer, Angel E García, B. Garcia-Moreno E., and Catherine A. Royer. Cavities determine the pressure unfolding of proteins., *Proceedings of the National Academy of Sciences of the United States of America*, 109(18):6945–6950, April 2012.
- [49] Lydia Nisius and Stephan Grzesiek. Key stabilizing elements of protein structure identified through pressure and temperature perturbation of its hydrogen bond network., *Nature chemistry*, 4(9):711–7, September 2012.
- [50] Erik van Dijk, Patrick Varilly, Tuomas P.J. Knowles, Daan Frenkel, and Sanne Abeln. Consistent treatment of hydrophobicity in protein lattice models accounts for cold denaturation, *Physical Review Letters*, 116(7):078101, February 2015.
- [51] Edgar Larios and Martin Gruebele. Protein stability at negative pressure., *Methods (San Diego, Calif.)*, 52(1):51–6, September 2010.
- [52] Harold W Hatch, Frank H Stillinger, and Pablo G. Debenedetti. Computational study of the stability of the miniprotein trp-cage, the GB1 β -hairpin, and the AK16 peptide, under negative pressure., *The journal of*

- physical chemistry. B, 118(28):7761–9, July 2014.
- [53] Simon A. Hawley. Reversible pressure-temperature denaturation of chymotrypsinogen, *Biochemistry*, 10(13):2436–2442, June 1971.
 - [54] Filip Meersman, László Smeller, and Karel Heremans. Protein stability and dynamics in the pressure-temperature plane., *Biochimica et biophysica acta*, 1764(3):346–54, March 2006.
 - [55] Kevin Stokely, Marco G Mazza, H. Eugene Stanley, and Giancarlo Franzese. Effect of hydrogen bond cooperativity on the behavior of water, *Proceedings of the National Academy of Sciences of the United States of America*, 107:1301–1306, 2010.
 - [56] Elena G Strelakova, Marco G Mazza, H. Eugene Stanley, and Giancarlo Franzese. Large Decrease of Fluctuations for Supercooled Water in Hydrophobic Nanoconfinement, *Physical Review Letters*, 106:145701, 2011.
 - [57] Giancarlo Franzese, Valentino Bianco, and Svilen Iskrov. Water at interface with proteins. *Food Biophysics*, 6:186–198, 2011.
 - [58] Marco G Mazza, Kevin Stokely, Sara E Pagnotta, Fabio Bruni, H. Eugene Stanley, and Giancarlo Franzese. More than one dynamic crossover in protein hydration water, *Proceedings of the National Academy of Sciences*, 108(50):19873–19878, 2011.
 - [59] Valentino Bianco, Oriol Vilanova, and Giancarlo Franzese. Polyamorphism and polymorphism of a confined water monolayer: liquid-liquid critical point, liquid-crystal and crystal-crystal phase transitions, *Proceedings of Perspectives and Challenges in Statistical Physics and Complex Systems for the Next Decade: A Conference in Honor of Eugene Stanley and Liacir Lucen*, pages 126–149, 2013.
 - [60] Francisco de los Santos and Giancarlo Franzese. Understanding Diffusion and Density Anomaly in a Coarse-Grained Model for Water Confined between Hydrophobic Walls, *The Journal of Physical Chemistry B*, 2011.
 - [61] Valentino Bianco and Giancarlo Franzese. Critical behavior of a water monolayer under hydrophobic confinement, *Scientific Reports*, 4:4440, April 2014.
 - [62] Luis Enrique Coronas, Valentino Bianco, Arne Zantop, and Giancarlo Franzese. Liquid-Liquid Critical Point in 3D Many-Body Water Model, *ArXiv* <https://arxiv.org/abs/1610.00419>, October 2016.
 - [63] Dario Corradini and Paola Gallo. Liquid-Liquid Coexistence in NaCl Aqueous Solutions: A Simulation Study of Concentration Effects, *The Journal of Physical Chemistry B*, 115(48):14161–14166, 2011.
 - [64] Lisandro, Hernández de la Peña and Peter G Kusalik. Temperature Dependence of Quantum Effects in Liquid Water, *Journal of the American Chemical Society*, 127(14):5246–5251, 2005.
 - [65] Alan K. Soper and Maria Antonietta Ricci. Structures of high-density and low-density water, *Physical Review Letters*, 84(13):2881–2884, March 2000.
 - [66] Kit Fun Lau and Ken A Dill. A lattice statistical mechanics model of the conformational and sequence spaces of proteins, *Macromolecules*, 22(10):3986–3997, 1989.
 - [67] Guido Caldarelli and Paolo, De Los Rios, Cold and Warm Denaturation of Proteins, *Journal of Biological Physics*, 27(2-3):229–241, 2001.
 - [68] Cristiano L Dias, Tapio Ala-Nissila, Mikko Karttunen, Ilpo Vattulainen, and Martin Grant. Microscopic Mechanism for Cold Denaturation, *Physical Review Letters*, 100(11):118101–118104, 2008.
 - [69] Christian Leth Petersen, Klaas-Jan Tielrooij, and Huib J. Bakker. Strong temperature dependence of water reorientation in hydrophobic hydration shells., *The Journal of chemical physics*, 130(21):214511, June 2009.
 - [70] Sapna Sarupria and Shekhar Garde. Quantifying Water Density Fluctuations and Compressibility of Hydration Shells of Hydrophobic Solutes and Proteins, *Phys. Rev. Lett.*, 103(3):37803, 2009.
 - [71] Yu. I. Tarasevich. State and structure of water in vicinity of hydrophobic surfaces, *Colloid Journal*, 73(2):257–266, April 2011.
 - [72] Joel G. Davis, Kamil P. Gierszal, Ping Wang, and Dor Ben-Amotz. Water structural transformation at molecular hydrophobic interfaces, *Nature*, 491(7425):582–585, November 2012.
 - [73] Norbert Muller. Search for a realistic view of hydrophobic effects, *Accounts of Chemical Research*, 23(1):23–28, 1990.
 - [74] Ka Lum, David Chandler, and John D Weeks. Hydrophobicity at Small and Large Length Scales, *The Journal of Physical Chemistry B*, 103(22):4570–4577, 1999.
 - [75] D Schwendel, T Hayashi, R Dahint, A Pertsin, M Grunze, R Steitz, and F Schreiber. Interaction of Water with Self-Assembled Monolayers: Neutron Reflectivity Measurements of the Water Density in the Interface Region, *Langmuir*, 19(6):2284–2293, 2003.
 - [76] Torben R Jensen, Morten, Ostergaard Jensen, Niels Reitzel, Konstantin Balashev, Günther H Peters, Kristian Kjaer, and Thomas Bjørnholm. Water in Contact with Extended Hydrophobic Surfaces: Direct Evidence of Weak Dewetting, *Phys. Rev. Lett.*, 90(8):86101, February 2003.
 - [77] Dhaval A Doshi, Erik B Watkins, Jacob N Israelachvili, and Jaroslaw Majewski. Reduced water density at hydrophobic surfaces: Effect of dissolved gases, *Proceedings of the National Academy of Sciences of the United States of America*, 102(27):9458–9462, 2005.
 - [78] Rahul Godawat, Sumanth N Jamadagni, and Shekhar Garde. Characterizing hydrophobicity of interfaces by using cavity formation, solute binding, and water correlations., *Proceedings of the National Academy of Sciences of the United States of America*, 106(36):15119–24, October 2009.
 - [79] Tuhin Ghosh, Angel E García, and Shekhar Garde. Molecular Dynamics Simulations of Pressure Effects on Hydrophobic Interactions, *Journal of the American Chemical Society*, 123(44):10997–11003, 2001.
 - [80] Cristiano L Dias and Hue Sun Chan. Pressure-Dependent Properties of Elementary Hydrophobic Interactions: Ramifications for Activation Properties of Protein Folding., *The journal of physical chemistry. B*, 118(27):7488–7509, June 2014.
 - [81] Valentino Bianco, Neus Pagès Gelabert, Ivan Coluzza, and Giancarlo Franzese. How the stability of a folded protein depends on interfacial water properties and residue-residue interactions, *ArXiv e-prints*, April 2017.
 - [82] Daan Frenkel and Berend Smit, *Understand molecular simulations*, Academic Press, San Diego, London, 2002.
 - [83] Marc Habash and Gregor Reid. Microbial biofilms: their development and significance for medical device-related infections., *J. Clin. Pharmacol.*, 39(9):887–898, 1999.

- [84] Anna Salvati, Andrzej S. Pitek, Marco P. Monopoli, Kanlaya Prapainop, Francesca Baldelli Bombelli, Delyan R. Hristov, Philip M. Kelly, Christoffer Åberg, Eugene Mahon, and Kenneth A. Dawson. Transferrin-functionalized nanoparticles lose their targeting capabilities when a biomolecule corona adsorbs on the surface., *Nat. Nanotechnol.*, 8(2):137–143, feb 2013.
- [85] Hong-ming Ding and Yu-qiang Ma. Design strategy of surface decoration for efficient delivery of nanoparticles by computer simulation, *Sci. Rep.*, 6(May):26783, 2016.
- [86] Alfonso De Simone, Roberta Spadaccini, Piero A. Temussi, and Franca Fraternali. Toward the understanding of MNEI sweetness from hydration map surfaces, *Biophys. J.*, 90(9):3052–3061, 2006.
- [87] Víctor F. Puentes. Design and pharmacokinetic aspects for the use of inorganic nanoparticles in radiomedicine, *Br. J. Radiol.*, 89(1057):20150210, 2016.
- [88] Stina Lindman, Iseult Lynch, Eva Thulin, Hanna Nilsson, Kenneth A. Dawson, and Sara Linse. Systematic investigation of the thermodynamics of HSA adsorption to N-iso-propylacrylamide/N-tert-butylacrylamide copolymer nanoparticles. Effects of particle size and hydrophobicity, *Nano Lett.*, 7(4):914–920, 2007.
- [89] Kenneth A. Dawson, Anna Salvati, and Iseult Lynch. Nanotoxicology: Nanoparticles reconstruct lipids. *Nat Nano*, 4(2):84–85, 02 2009.
- [90] Martin Lundqvist, Johannes Stigler, Giuliano Elia, Iseult Lynch, Tommy Cedervall, and Kenneth A. Dawson. Nanoparticle size and surface properties determine the protein corona with possible implications for biological impacts. *Proceedings of the National Academy of Sciences*, 105(38):14265–14270, 09 2008.
- [91] N. Pratap, A. Casey, Lynch I. Tenuta, T., and K. A. Dawson. Preparation, characterization and ecotoxicological evaluation of four environmentally relevant species of n- isopropylacrylamide and n- isopropylacrylamide-co-n-tert-butylacrylamide copolymer nanoparticles. *Aquatic Toxicology*, 92:146–154, 2009.
- [92] Pilar, Rivera Gil, Günter Oberdörster, Alison Elder, Víctor F. Puentes, and Wolfgang J. Parak. Correlating physico-chemical with toxicological properties of nanoparticles: The present and the future, *ACS Nano*, 4(10):5227–5231, 2010.
- [93] Claudia Corbo, Roberto Molinaro, Alessandro Parodi, Naama E. Toledano Furman, Francesco Salvatore, and Ennio Tasciotti. The impact of nanoparticle protein corona on cytotoxicity, immunotoxicity and target drug delivery, *Nanomedicine*, 11(1):81–100, 2016.
- [94] Iseult Lynch, Tommy Cedervall, Martin Lundqvist, Celia Cabaleiro-Lago, Sara Linse, and Kenneth A. Dawson. The nanoparticle–protein complex as a biological entity; a complex fluids and surface science challenge for the 21st century. *Advances in Colloid and Interface Science*, 134–135(0):167–174, 10 2007.
- [95] Tommy Cedervall, Iseult Lynch, Stina Lindman, Tord Berggård, Eva Thulin, Hanna Nilsson, Kenneth A. Dawson, and Sara Linse. Understanding the nanoparticle-protein corona using methods to quantify exchange rates and affinities of proteins for nanoparticles., *Proc. Natl. Acad. Sci. U. S. A.*, 104(7):2050–2055, 2007.
- [96] Iseult Lynch, Anna Salvati, and Kenneth A. Dawson. Protein-nanoparticle interactions: What does the cell see?, *Nat. Nanotechnol.*, 4(9):546–547, 2009.
- [97] Dorota Walczyk, Francesca Baldelli Bombelli, Marco P. Monopoli, Iseult Lynch, and Kenneth A. Dawson. What the cell “sees” in bionanoscience., *J. Am. Chem. Soc.*, 132(16):5761–5768, apr 2010.
- [98] Eudald Casals, Tobias Pfaller, Albert Duschl, Gertie Janneke Oostingh, and Víctor F. Puentes. Time evolution of the nanoparticle protein corona, *ACS Nano*, 4(7):3623–3632, 2010.
- [99] Daniele Dell’Orco, Martin Lundqvist, Cecilia Oslakovic, Tommy Cedervall, and Sara Linse. Modeling the time evolution of the nanoparticle-protein corona in a body fluid, *PLoS One*, 5(6):e10949, 2010.
- [100] Silvia Milani, Francesca Baldelli Bombelli, Andrzej S. Pitek, Kenneth A. Dawson, Joachim Rädler, and Francesca Baldelli Bombelli. Reversible versus irreversible binding of transferrin to polystyrene nanoparticles: soft and hard corona., *ACS Nano*, 6(3):2532–2541, mar 2012.
- [101] Andrzej S. Pitek, D. O’Connell, Eugene Mahon, Marco P. Monopoli, Francesca Baldelli Bombelli, and Kenneth A. Dawson. Transferrin Coated Nanoparticles: Study of the Bionano Interface in Human Plasma, *PLoS One*, 7(7):e40685, 2012.
- [102] Marco P. Monopoli, Christoffer Åberg, Anna Salvati, and Kenneth A. Dawson. Biomolecular coronas provide the biological identity of nanosized materials., *Nat. Nanotechnol.*, 7(12):779–786, dec 2012.
- [103] Martin Lundqvist, Johannes Stigler, Tommy Cedervall, Tord Berggård, Michelle B. Flanagan, Iseult Lynch, Giuliano Elia, and Kenneth Dawson. The evolution of the protein corona around nanoparticles: A test study. *ACS Nano*, 5(9):7503–7509, 2012/10/15 2011.
- [104] Kayle Shapero, Federico Fenaroli, Iseult Lynch, David C. Cottell, Anna Salvati, and Kenneth A. Dawson. Time and space resolved uptake study of silica nanoparticles by human cells. *Mol. BioSyst.*, 7:371–378, 2011.
- [105] Anna Salvati, Christoffer Åberg, Tiago dos Santos, Juan Varela, Paulo Pinto, Iseult Lynch, and Kenneth A. Dawson. Experimental and theoretical comparison of intracellular import of polymeric nanoparticles and small molecules: toward models of uptake kinetics. *Nanomedicine: Nanotechnology, Biology and Medicine*, 7(6):818–826, 12 2011.
- [106] Marco P. Monopoli, Dorota Walczyk, Abigail Campbell, Giuliano Elia, Iseult Lynch, Francesca Baldelli Bombelli, and Kenneth A. Dawson. Physical-chemical aspects of protein corona: relevance to in vitro and in vivo biological impacts of nanoparticles., *J. Am. Chem. Soc.*, 133(8):2525–2534, mar 2011.
- [107] Marco P. Monopoli, Francesca Baldelli Bombelli, and Kenneth A. Dawson. Nanobiotechnology: Nanoparticle coronas take shape. *Nat Nano*, 6(1):11–12, 01 2011.
- [108] Pol Vilaseca, Kenneth A. Dawson, and Giancarlo Franzese. Understanding and modulating the competitive surface-adsorption of proteins through coarse-grained molecular dynamics simulations, *Soft Matter*, 9(29):6978–6985, 2013.
- [109] Oriol Vilanova. Bionano interactions: Interactions between nanoscopic systems and biological macromolecules in solution PhD thesis, Universitat de Barcelona, 2017.
- [110] Oriol Vilanova, Judith J. Mittag, Philip M. Kelly, Silvia Milani, Kenneth A. Dawson, Joachim O. Rädler,

- and Giancarlo Franzese. Understanding the kinetics of protein–nanoparticle corona formation. *ACS Nano*, 10(12):10842–10850, 12 2016.
- [111] Pradeep Kumar, Giancarlo Franzese, and H. Eugene Stanley. Dynamics and thermodynamics of water, *J. Phys. Condens. Matter*, 20(24):244114, 2008.
 - [112] Marco G Mazza, Kevin Stokely, Elena G Strekalova, H. Eugene Stanley, and Giancarlo Franzese. Cluster Monte Carlo and numerical mean field analysis for the water liquid-liquid phase transition, *Computer Physics Communications*, 180(4):497–502, 2009.
 - [113] Giancarlo Franzese, G Malescio, A Skibinsky, Sergey V Buldyrev, and H. Eugene Stanley. Metastable liquid-liquid phase transition in a single-component system with only one crystal phase and no density anomaly, *Physical Review E*, 66(5):51206, November 2002.
 - [114] Giancarlo Franzese and H. Eugene Stanley. A theory for discriminating the mechanism responsible for the water density anomaly, *Phys. A Stat. Mech. its Appl.*, 314(1-4):508–513, nov 2002.
 - [115] Giancarlo Franzese and H. Eugene Stanley. Liquid-liquid critical point in a Hamiltonian model for water: analytic solution, *Journal of Physics: Condensed Matter*, 14(9):2201–2209, March 2002.
 - [116] <https://github.com/bubbles-suite/BUBBLES>, 2015.
 - [117] Giancarlo Franzese. Differences between discontinuous and continuous soft-core attractive potentials: The appearance of density anomaly. *Journal of Molecular Liquids*, 136(3):267–273, 12 2007.
 - [118] Pol Vilaseca and Giancarlo Franzese. Isotropic soft-core potentials with two characteristic length scales and anomalous behaviour, *Journal of Non-Crystalline Solids*, 357(2):419–426, 2011.
 - [119] Oriol Vilanova and Giancarlo Franzese. Structural and dynamical properties of nanoconfined supercooled water, *arXiv.org*, page arXiv:1102.2864, 2011.
 - [120] Valentino Bianco, Giancarlo Franzese, Christoph Delgado, and Ivan Coluzza. Role of water in the selection of stable proteins at ambient and extreme thermodynamic conditions. *Phys. Rev. X*, 7:021047, Jun 2017.